

Thermal Properties of $0.9\text{CaMgSi}_2\text{O}_6$ - 0.1MgSiO_3 Glass-Ceramics

Chang Jun Jeon, Gui Nam Sun, Jong Kyu Lee, Han Sae Ju, and Eung Soo Kim[†]

Department of Materials Engineering, Kyonggi University, Suwon 443-760, Korea

(Received October 25, 2011; Revised December 5, 2011, January 14, 2012; Accepted January 19, 2012)

ABSTRACT

Dependencies of thermal properties on the crystallization behavior of $0.9\text{CaMgSi}_2\text{O}_6$ - 0.1MgSiO_3 glass-ceramics were investigated as a function of heat-treatment temperature from 750°C to 950°C. The crystallization behavior of the specimens depended on the heat-treatment temperature, which could be evaluated by differential thermal analysis (DTA), Fourier transform infrared spectroscopy (FT-IR), and X-ray diffraction (XRD) analysis by the Rietveld-reference intensity ratio (RIR) combined procedure. With an increase of the heat-treatment temperature, the thermal conductivity and thermal diffusivity of the heat-treated specimens increased. These results could be attributed to the increase of crystallization with heat-treatment temperature. However, the specific heat capacity of the heat-treated specimens was not affected by the heat-treatment temperature. The thermal conductivities measured from 25°C to 100°C were also discussed for application to lighting-emitting diode (LED) packages and substrate materials.

Key words : Thermal properties, Glass-ceramics, Crystallization, Heat-treatment temperature

1. Introduction

Glass-ceramics are fine-grained polycrystalline materials obtained from a parent glass by controlled crystallization. The glass-ceramics of the CaO-MgO-SiO₂ system have been extensively investigated for industrial applications because they are common and inexpensive materials. Also, these materials present good chemical resistance, high mechanical properties, and a wide range of crystalline phases that result from the surface devitrification of single-step temperature treatment. Among the crystalline phases, diopside ($\text{CaMgSi}_2\text{O}_6$) and enstatite (MgSiO_3) phases are usually generated.

For multilayer packages applicable to lighting-emitting diodes (LED) with high-power, the diopside-enstatite system could be used due to its relatively low heat-treatment temperature and high thermal conductivity, which could make this material applicable in the process of co-firing with low-melting point electrodes (Ag = 960°C, Cu = 1050°C) and to obtain fast heat dissipations in LED chips.

In our preliminary experiment, the diopside-enstatite system of $0.9\text{CaMgSi}_2\text{O}_6$ - 0.1MgSiO_3 glass-ceramics heat-treated at 800°C for 5 h had thermal properties that were better than those of the other compositions of the $\text{CaMgSi}_2\text{O}_6$ - MgSiO_3 system. Since the thermal properties of the glass-ceramics were found to change with heat-treatment temperature due to changes of crystallization, the dependence of the thermal properties on the degree of crystallization of $0.9\text{CaMgSi}_2\text{O}_6$ - 0.1MgSiO_3 glass-ceramics should be investigated as a function

of heat-treatment conditions.

A number of techniques have been employed for the determination of the crystalline phase of glass-ceramics. The most commonly used methods are microscopy, chemical separation, density measurements, and X-ray diffraction.¹⁾ The main disadvantage of microscopy is that it is time-consuming. Also, chemical separation and density methods have drawbacks such as small differences of solubility or density between the crystalline phase and the residual glass. Therefore, the degree of crystallization should be evaluated from the XRD patterns using a combination of Rietveld and reference intensity ratio (RIR) methods.^{2,3)}

In this study, the effects of crystallization behavior on the thermal properties of $0.9\text{CaMgSi}_2\text{O}_6$ - 0.1MgSiO_3 glass-ceramics were investigated as a function of heat-treatment conditions. The crystallization behavior, such as degree of crystallization in glass-ceramics, was determined by a combined Rietveld-RIR procedure. The temperature coefficient of thermal conductivity (Tck) was also discussed for practical application to LED multilayer devices.

2. Experimental Procedure

High-purity oxide powders of CaCO₃ (99%, High Purity Chemicals, Japan), MgCO₃ (99.9%, High Purity Chemicals, Japan), and SiO₂ (99.9%, High Purity Chemicals, Japan) were used as starting powders. The powders were separately prepared according to the desired compositions of $\text{CaMgSi}_2\text{O}_6$ and MgSiO_3 , and grounded with ZrO₂ balls for 24 h in ethanol. The mixed powders were melted in a platinum crucible at 1500°C for 3 h and quenched into distilled water. The cullets were pulverized and mixed according to the desired formula of $0.9\text{CaMgSi}_2\text{O}_6$ -

[†]Corresponding author : Eung Soo Kim
E-mail : eskim@kyonggi.ac.kr
Tel : +82-31-249-9764 Fax : +82-31-244-6300

0.1MgSiO₃, and then melted again at 1500°C for 3 h. Pure glass frits were obtained by quenching of melts into distilled water. These glass frits were re-milled for 24 h and pressed into pellets isostatically under a pressure of 147 MPa. These pellets were heat-treated from 750°C to 950°C for 5 h in air.

The densities of the heat-treated specimens were measured by the Archimedes method. The differential thermal analysis (DTA) curve was obtained by a simultaneous thermal analyzer-mass spectrometer (STA 409PC-QMS 403C, NETZSCH, Germany) at different heating rates (5–20°C/min). Fourier transform infrared spectroscopy (FT-IR, FT/IR-430, JASCO, Japan) and powder X-ray diffraction analysis (XRD, D/Max-2500V/PC, RIGAKU, Japan) were used to evaluate the crystallization behaviors of the glass samples, the network structures and crystalline phases of glass-ceramics.

The degree of crystallization of the heat-treated specimens was obtained by the combined Rietveld and reference intensity ratio (RIR) methods.^{2,3} A 10 wt% sample of α-Al₂O₃ (annealed at 1500°C for 1 day to increase the crystallinity to 100 wt%) was added to all specimens as an internal standard.³ Rietveld refinements of the XRD patterns were performed using the Full-Prof program.⁴ The initial structure models for CaMgSi₂O₆ and α-Al₂O₃ compounds were taken from the previous reports.^{5,6} The degree of crystallization (α) of the specimens in relation to the internal standard was evaluated from Eq. (1).²

$$\alpha = (W_c/W_{std}) \times (W_{std}/W) \quad (1)$$

where W , W_c , and W_{std} are the weights of the specimens, the crystalline component, and the internal standard, respectively. The value of W_c/W_{std} was calculated by Rietveld quantitative analysis under the condition of $W_c + W_{std} = 1$, and W_{std}/W was obtained by measuring the weights of the specimens and the internal standard.²

The thermal properties (thermal conductivity, thermal diffusivity, and specific heat capacity) were measured by a laser flash apparatus (LFA 457, NETZSCH, Germany). The temperature dependence of the thermal conductivity was measured in the temperature range from 25°C to 100°C.

3. Results and Discussion

Fig. 1 shows the differential thermal analysis (DTA) curves of (1-x)CaMgSi₂O₆-xMgSiO₃ glass powders with different heating rates. The strong exothermic reactions that peaked at 875–900°C are attributed to the crystallization of glass at each heating rate. For the glass powders with the same heating rate of 20°C/min (Fig. 1(d) and (e)), the peak temperature of crystallization (T_p) of 0.9CaMgSi₂O₆-0.1MgSiO₃ glass was lower than that of 0.52CaMgSi₂O₆-0.48MgSiO₃ glass. With an increase of heating rate (Fig. 1(a)–(d)), the T_p values of glasses shifted to higher temperatures. From the T_p values of glasses with different heating rates, the activation energy of crystallization (E_a) was calculated using the following modified forms of the Kissinger (Eq. (2)) and Ozawa (Eq. (3)) Equations.

$$\ln (T_p^2/\beta^n) = (E_a/RT_p) + \text{constant} \quad (2)$$

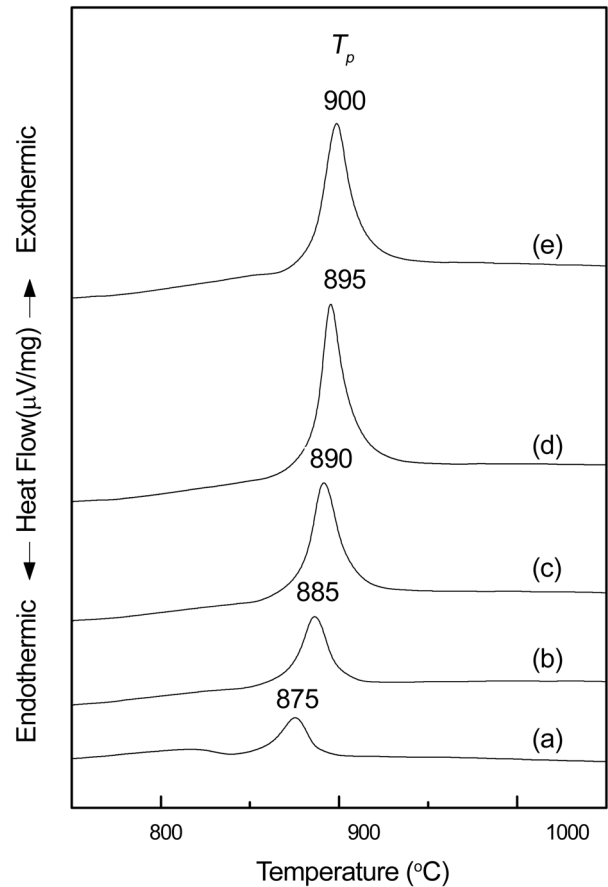


Fig. 1. DTA curves of (1-x)CaMgSi₂O₆-xMgSiO₃ glass powders with different heating rates; (a) $x = 0.1$, 5°C/min, (b) $x = 0.1$, 10°C/min, (c) $x = 0.1$, 15°C/min, (d) $x = 0.1$, 20°C/min, (e) $x = 0.42$, 20°C/min.

$$\ln \beta = -mE_a/nRT_p + \text{constant} \quad (3)$$

where β is the heating rate (5–20°C/min), R is the ideal gas constant, n is the Avrami constant, and m is the crystal growth dimensionality. It has been reported⁷ that nucleation does not occur during crystal growth and that crystal growth is interface controlled. In this study, the values of n and m were considered both to be equal to 1, which is the case for surface crystallization⁷, because CaMgSi₂O₆ and MgSiO₃ were generally generated from the surface crystallization.^{8,9} The values of $\ln (T_p^2/\beta)$ versus $1/T_p$ and $\ln \beta$ versus $1/T_p$ were plotted from T_p and β . The E_a values of Kissinger (785 kJ/mol) and Ozawa (804 kJ/mol) were obtained from the slope of the solid line by least squares fitting of the data points. The similar E_a values of Kissinger and Ozawa imply the weak dependence of T_p on the heating rate.¹⁰ These E_a values of the diopside-enstatite system were larger than those (Kissinger = 507 kJ/mol, Ozawa = 501 kJ/mol) of diopside based glass-ceramics reported by Goel *et al.*⁸ due to the E_a values of enstatite, which were larger than those of diopside.⁹

To investigate the dependence of the thermal properties on the crystallization behaviors of (1-x)CaMgSi₂O₆-xMgSiO₃

glasses, the heat-treatment temperatures from 750°C to 950°C were determined from the results of the DTA data.

Fig. 2 shows the FT-IR spectra of $0.9\text{CaMgSi}_2\text{O}_6\text{-}0.1\text{MgSiO}_3$ specimens heat-treated from 750°C and 950°C for 5 h. The specimens heat-treated at 750°C showed three broad bands similar to those observed for the parent glass powders,¹¹ which indicated the amorphous nature of the specimens. With an increase of the heat-treatment temperature to 800°C, the three broad transmittance bands split into a number of intense and sharp bands due to the increase of crystallization of the specimens.¹¹ For further increase of the heat-treatment temperature, however, the bands showed similar intensities. For $0.9\text{CaMgSi}_2\text{O}_6\text{-}0.1\text{MgSiO}_3$ specimens heat-treated from 800°C to 950°C (Fig. 2(b)-(e)), the bands in the region of 400-1200 cm^{-1} for diopside ($\text{CaMgSi}_2\text{O}_6$) were confirmed to be in accordance with those in the report of Omori.¹² The transmittance bands in the 400-600 cm^{-1} and 600-800 cm^{-1} regions are due to the bending vibrations of O-Mg-O and O-Si-O linkages with non-bridging oxygen atoms, respectively. The broad bands in the 800-1300 cm^{-1} are assigned to the stretching vibrations of the SiO_4 tetrahedron with different numbers of non-bridging and bridging oxygen atoms. For the specimens heat-treated at the

temperature of 950°C (Fig. 2(e) and (f)), $0.52\text{CaMgSi}_2\text{O}_6\text{-}0.48\text{MgSiO}_3$ showed smaller intensities of bands than did $0.9\text{CaMgSi}_2\text{O}_6\text{-}0.1\text{MgSiO}_3$. A new band at 705 cm^{-1} was observed for $0.52\text{CaMgSi}_2\text{O}_6\text{-}0.48\text{MgSiO}_3$ specimens heat-treated at 950°C.

From the results of DTA curves and FT-IR spectra, the physical and thermal properties of the $0.9\text{CaMgSi}_2\text{O}_6\text{-}0.1\text{MgSiO}_3$ glass-ceramics were investigated because it has lower value of T_p and larger intensities of bands (higher degree of crystallization) than those characteristics of the $0.52\text{CaMgSi}_2\text{O}_6\text{-}0.48\text{MgSiO}_3$ glass-ceramics.

The apparent and relative densities of $0.9\text{CaMgSi}_2\text{O}_6\text{-}0.1\text{MgSiO}_3$ specimens heat-treated from 750°C and 950°C for 5 h are summarized in Table 1. With an increase of heat-treatment temperature from 750°C to 950°C, the apparent and relative densities of the specimens remarkably increased up to 800°C, and then were almost constant.

Fig. 3 provides SEM micrographs of $0.9\text{CaMgSi}_2\text{O}_6\text{-}0.1\text{MgSiO}_3$ specimens heat-treated from 750°C to 950°C for 5 h. The porosity of the specimens heat-treated at 750°C was larger than that of the specimens heat-treated from 800°C to 950°C;

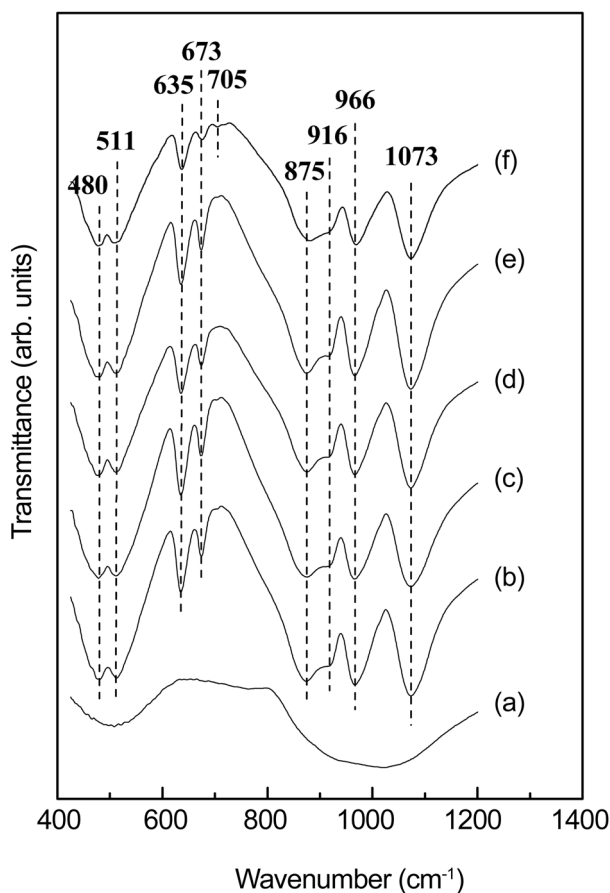


Fig. 2. FT-IR spectra of $(1-x)\text{CaMgSi}_2\text{O}_6\text{-}x\text{MgSiO}_3$ specimens with various heat-treatment temperatures; (a) $x = 0.1$, 750°C-5 h, (b) $x = 0.1$, 800°C-5 h, (c) $x = 0.1$, 850°C-5 h, (d) $x = 0.1$, 900°C-5 h, (e) $x = 0.1$, 950°C-5 h, (f) $x = 0.42$, 950°C-5 h.

Table 1. Apparent density, relative density, and crystallite size of $0.9\text{CaMgSi}_2\text{O}_6\text{-}0.1\text{MgSiO}_3$ specimens heat-treated from 750°C to 950°C for 5 h

Heat-Treatment Temperature (°C)	Apparent Density (g/cm^3)	Relative Density (%)	Crystallite Size (nm)
750	2.705	83.02	-
800	2.970	91.15	28.48
850	2.964	90.97	27.40
900	2.966	91.03	29.44
950	2.969	91.12	32.86

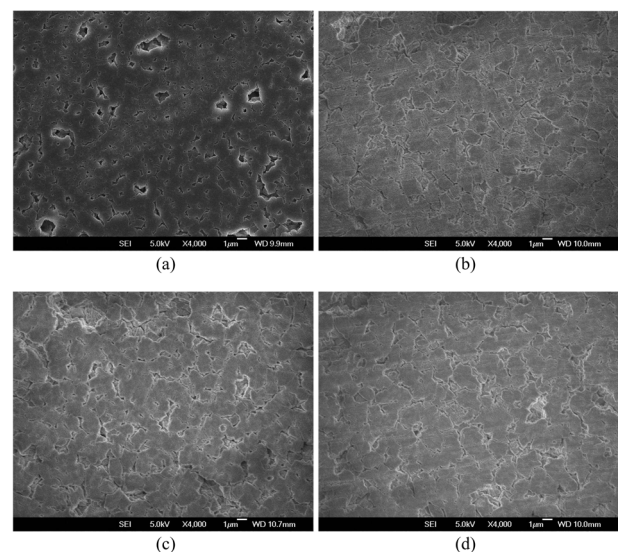


Fig. 3. SEM micrographs of $0.9\text{CaMgSi}_2\text{O}_6\text{-}0.1\text{MgSiO}_3$ specimens heat-treated at 750°C, (b) 800°C, (c) 850°C, and (d) 950°C for 5 h (bar = 1 μm).

results for density were similar (Table 1). However, the crystalline diopside ($\text{CaMgSi}_2\text{O}_6$) was not observed.

XRD patterns of $0.9\text{CaMgSi}_2\text{O}_6\text{-}0.1\text{MgSiO}_3$ specimens heat-treated from 750°C and 950°C for 5 h are shown in Fig. 4.

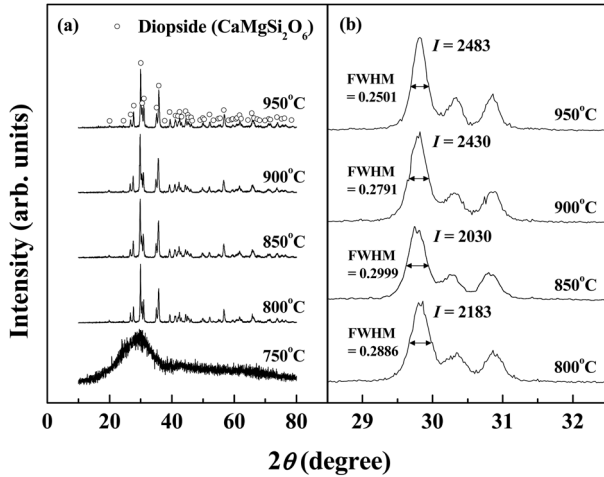


Fig. 4. XRD patterns of $0.9\text{CaMgSi}_2\text{O}_6\text{-}0.1\text{MgSiO}_3$ specimens heat-treated from 750°C to 950°C for 5 h; (a) $2\theta = 10\text{-}80^\circ$, (b) $2\theta = 29\text{-}32^\circ$.

The XRD pattern of specimens heat-treated at 750°C showed the typical amorphous halo (Fig. 4(a)). However, the single phase with monoclinic diopside ($\text{CaMgSi}_2\text{O}_6$) structure was confirmed for the specimens heat-treated from 800°C to 950°C . These results are in agreement with the results of the FT-IR spectra given in Fig. 2. With an increase of the heat-treatment temperature from 800°C to 950°C , the intensity (I) of the main peak at $2\theta = 29.8^\circ$ decreased up to 850°C and then increased, while the full width at half maximum intensity (FWHM) increased up to 850°C and then decreased (Fig. 4(b)). The crystallite size (L) of the specimens was calculated from the FWHM using Scherrer's Equation.¹³⁾ With an increase of heat-treatment temperature from 800°C to 950°C , the L of the specimens decreased up to 850°C and then increased, as can be seen in Table 1.

Fig. 5 shows the Rietveld refinement plots of the XRD data for the specimens heat-treated from 800°C to 950°C for 5 h. Dots are observed intensities, overlying solid lines are calculated intensities, and bottom lines are the difference between the observed and calculated intensities. Short vertical bars indicate the Bragg reflections that were allowed for the monoclinic diopside (top) and rhombohedral $\alpha\text{-Al}_2\text{O}_3$ (bottom) phases. All peaks in the XRD patterns fit well with the mon-

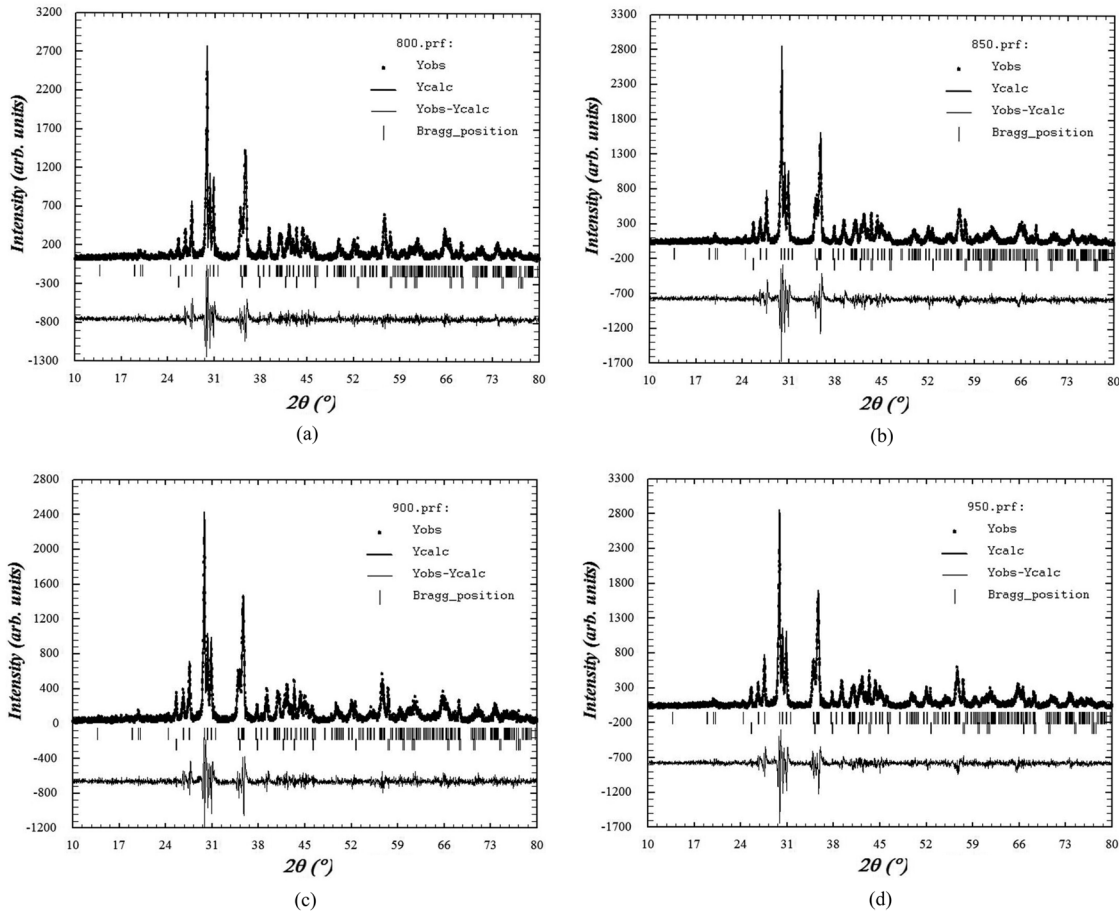


Fig. 5. Rietveld refinement patterns of $0.9\text{CaMgSi}_2\text{O}_6\text{-}0.1\text{MgSiO}_3$ specimens heat-treated from 800°C to 950°C for 5 h; (a) 800°C , (b) 850°C , (c) 900°C , and (d) 950°C .

monoclinic diopside (*C12/c1*)⁵ and rhombohedral α -Al₂O₃ (*R-3cH*)⁶ structures. The degree of crystallization and Bragg R-factor obtained from the Rietveld-RIR quantitative analysis of XRD data are summarized in Table 2. With an increase of heat-treatment temperature, the degree of crystallization decreased up to 850°C and then increased. The specimens heat-treated at 800°C showed a higher degree of crystallization than did the specimens heat-treated at 850°C. These results could be attributed to the crystallite size (Table 1).¹⁴ The validity of the Rietveld-RIR quantitative analysis was supported by the low values of the Bragg R-factors for each specimen.

Fig. 6 shows the thermal conductivity and specific heat capacity of 0.9CaMgSi₂O₆-0.1MgSiO₃ specimens heat-treated from 750°C and 950°C for 5 h. The specimens heat-treated at different temperatures showed similar values of specific heat capacity. In our preliminary results, a similar tendency was confirmed for the (1-x)CaMgSi₂O₆-xMgSiO₃ system. With an

Table 2. Degree of crystallization and Bragg R-factor of 0.9CaMgSi₂O₆-0.1MgSiO₃ specimens heat-treated from 800°C to 950°C for 5 h

		Heat-Treatment Temperature (°C)			
		800	850	900	950
Degree of Crystallization (%)		95.3	93.5	95.7	97.5
Bragg R-Factor (%)	Diopside	9.67	9.04	9.48	8.20
	α -Al ₂ O ₃	7.31	4.78	8.50	4.68

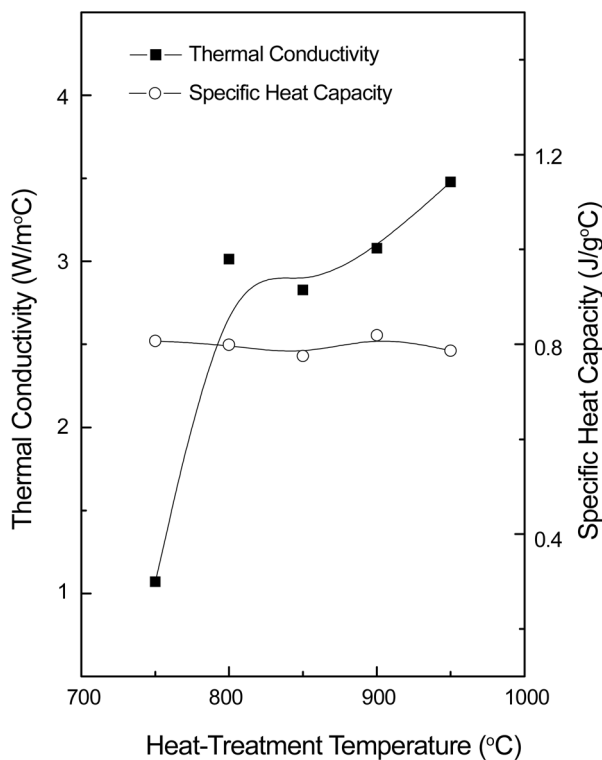


Fig. 6. Thermal conductivity and specific heat capacity of 0.9CaMgSi₂O₆-0.1MgSiO₃ specimens heat-treated from 750°C to 950°C for 5 h.

increase of heat-treatment temperature, the thermal conductivity of the specimens increased. With the heat-treatment temperature, the thermal diffusivity of the specimens showed a tendency similar to that of the thermal conductivity. The noticeable increases of thermal conductivity of the specimens heat-treated at 800°C were affected by the increase of density (Table 1), which could be attributed to the crystallization of glasses (Figs. 2 and 4), because the density of the crystalline phase (3.27 g/cm³) is higher than that of the amorphous phase (2.75 g/cm³).¹⁵ However, the thermal properties of the crystalline specimens heat-treated from 800°C to 950°C were not dependent on the density of the specimens due to the specimens' similar values of density (Table 1). Therefore, the precise degree of crystallization obtained from the combined Rietveld-RIR quantitative analysis should be considered for prediction of the thermal properties of glass-ceramics with crystalline phases.

Fig. 7 shows the dependence of thermal conductivity on the degree of crystallization of 0.9CaMgSi₂O₆-0.1MgSiO₃ specimens heat-treated from 800°C and 950°C for 5 h. With an increase of heat-treatment temperature, the thermal conductivity of the specimens decreased up to 850°C and then increased. These results are due to the degree of crystallization. It has been reported¹⁶ that the thermal conductivity of the crystal

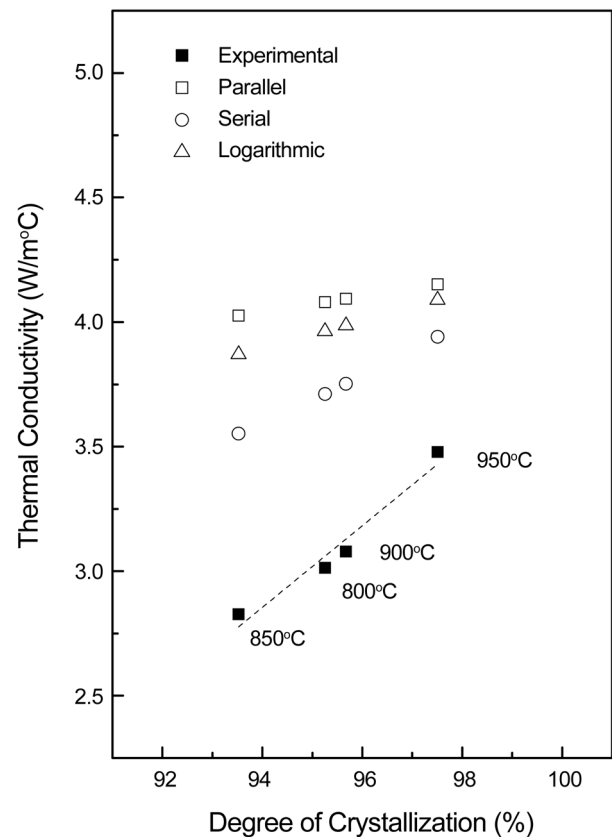


Fig. 7. Dependence of thermal conductivity on degree of crystallization of 0.9CaMgSi₂O₆-0.1MgSiO₃ specimens heat-treated from 800°C to 950°C for 5 h.

is larger than that of the glass in the glass system of $\text{CaO-SiO}_2\text{-Al}_2\text{O}_3\text{-MgO-Na}_2\text{O-B}_2\text{O}_3$. Considering the similar densities of the specimens heat-treated from 800°C to 950°C (Table 1) and the difference of the thermal conductivities between the amorphous phase (1.07 W/m°C) and the crystalline phase (4.23 W/m°C)¹⁷ of diopside, the dependence of thermal conductivity on the degree of crystallization could be evaluated by the general mixture models (parallel, serial, and logarithmic). Although the experimental thermal conductivities were lower than those obtained from general mixture models due to the relative densities of 90-91%, the thermal conductivities were found to increase with the degree of crystallization of the specimens, as can be seen in Fig. 7.

From the view point of practical application to LED multilayer devices, the change of thermal conductivity with temperature is a very important factor that can dissipate heat effectively, which dissipation can be evaluated by the temperature coefficient of the thermal conductivity (*Tck*) from 25°C to 100°C, as shown in Eq. (4).¹⁴

$$Tck = (k_{100^\circ\text{C}} - k_{25^\circ\text{C}}) / [(100^\circ\text{C} - 25^\circ\text{C}) \times k_{25^\circ\text{C}}] \quad (4)$$

where $k_{100^\circ\text{C}}$ and $k_{25^\circ\text{C}}$ are the thermal conductivities of the specimens measured at 100°C and 25°C, respectively.

Fig. 8 shows the *Tck* of $0.9\text{CaMgSi}_2\text{O}_6\text{-}0.1\text{MgSiO}_3$ specimens

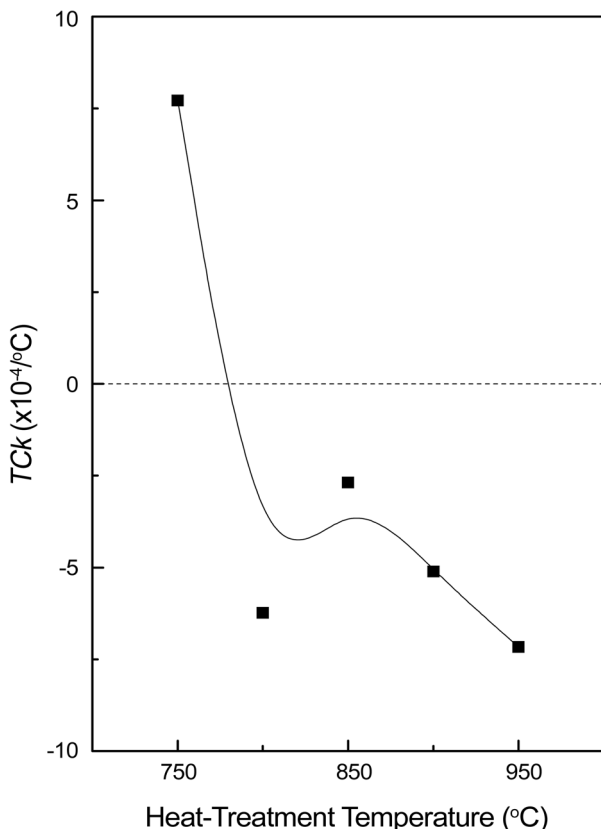


Fig. 8. Thermal coefficient of thermal conductivity (*Tck*) of $0.9\text{CaMgSi}_2\text{O}_6\text{-}0.1\text{MgSiO}_3$ specimens heat-treated from 750°C to 950°C for 5 h.

heat-treated from 750°C and 950°C for 5 h. With an increase of the heat-treatment temperature, the *Tck* values of the specimens changed from positive to negative due to the difference of the amorphous and crystalline phases, as confirmed in Figs. 2 and 4. In general, the thermal conductivity can be determined from the thermal diffusivity, specific heat capacity, and density.¹⁴ Similar values (0.8-0.9 J/g°C) of specific heat capacity measured at 100°C and 25°C were obtained for all of the specimens. However, the differences of thermal diffusivity values at 100°C from those at 25°C were affected by the heat-treatment temperature; typically, the differences of thermal diffusivity values at 100°C from those at 25°C were 0.06 mm²/s for the specimens heat-treated at 750°C and -0.14 mm²/s for the specimens heat-treated at 800°C. Therefore, the decrease of *Tck* of the specimens heat-treated at 800°C is due to the decrease of thermal diffusivity with the measuring temperature. A large positive *Tck* is preferred because it can dissipate effectively the heat generated from LED chips of multi-chip packages. Although the specimens heat-treated at 750°C showed a positive *Tck*, the thermal conductivity was very low. Also, a near zero value of *Tck* is required for the thermal stability of the specimens with high thermal conductivity. Good stability of thermal conductivity (near zero *Tck*) was obtained for specimens heat-treated at 850°C for 5 h.

4. Conclusions

With an increase of heat-treatment temperature from 750°C to 950°C for 5 h, the thermal conductivity and thermal diffusivity of the specimens increased, while the specific heat capacity of the specimens was not changed. For the specimens heat-treated at 800°C for 5 h, the remarkable increases of thermal conductivity and thermal diffusivity are due to the increase of density due to the crystallization of the glasses. The thermal conductivities of the specimens heat-treated from 800°C to 950°C for 5 h were dependent on the degree of crystallization of the diopside phase. The optimal degree of crystallization (97.5%) was obtained for the specimens heat-treated at 950°C for 5 h. The specimens heat-treated at 850°C for 5 h showed good thermal stability of thermal conductivity, which could be useful in practical applications.

Acknowledgments

This work was supported by the Human Resources Development of the Korea Institute of Energy Technology Evaluation and Planning (KETEP) grant funded by the Korea government Ministry of Knowledge Economy.

REFERENCES

1. H. S. Kim, R. D. Rawlings, and P. S. Rogers, "Quantitative Determination of Crystalline and Amorphous Phases in Glass-Ceramics by X-ray Diffraction Analysis," *Br. Ceram. Trans. J.*, **88** 21-5 (1989).

2. K. Yasukawa, Y. Terashi, and A. Nakayama, "Crystallinity Analysis of Glass-Ceramics by the Rietveld Method," *J. Am. Ceram. Soc.*, **81** 2978-82 (1998).
3. L. Barbieri, F. Bondioli, I. Lancellotti, C. Leonelli, M. Montorsi, A. M. Ferrari, and P. Miselli, "The Anorthite-Diopside System: Structural and Devitrification Study. Part II: Crystallinity Analysis by the Rietveld-RIR Method," *J. Am. Ceram. Soc.*, **88** 3131-6 (2005).
4. T. Roisnel and J. R. Carvajal, "WinPLOTR: A Windows Tool for Powder Diffraction Patterns Analysis," *Mat. Sci. Forum*, **378-81** 118-23 (2001).
5. J. R. Clark, D. E. Appleman, and J. J. Papike, "Crystal-Chemical Characterization of Clinopyroxenes Based on Eight New Structure Refinements," *Mineral. Soc. Amer. Spec. Pap.*, **2** 31-50 (1969).
6. N. Ishizawa, T. Miyata, I. Minato, F. Marumo, and S. Iwai, "A Structural Investigation of α -Al₂O₃ at 2170 K," *Acta Cryst.*, **B36** 228-30 (1980).
7. K. Matusita and S. Sakka, "Kinetic Study of Crystallization of Glass by Differential Thermal Analysis-Criterion on Application of Kissinger Plot," *J. Non-Cryst. Solids*, **38-9** 741-6 (1980).
8. A. Goel, D. U. Tulyaganov, V. V. Kharton, A. A. Yaremchenko, and J. M. F. Ferreira, "The Effect of Cr₂O₃ Addition on Crystallization and Properties of La₂O₃-Containing Diopside Glass-Ceramics," *Acta Mater.*, **56** 3065-76 (2008).
9. A. Goel, D. U. Tulyaganov, E. R. Shaaban, C. S. Knee, S. Eriksson, and J. M. F. Ferreira, "Structure and Crystallization Behaviour of Some MgSiO₃-Based Glasses," *Ceram. Int.*, **35** 1529-38 (2009).
10. P. J. Hayward, E. R. Vance, and D. C. Doern, "DTA/SEM Study of Crystallization in Sphene Glass-Ceramics," *Am. Ceram. Soc. Bull.*, **66** 1620-6 (1987).
11. A. Goel, R. Shaaban, D. U. Tulyaganov, and J. M. F. Ferreira, "Study of Crystallization Kinetics in Glasses along the Diopside-Ca-Tschermak Join," *J. Am. Ceram. Soc.*, **91** 2690-7 (2008).
12. K. Omori, "Analysis of the Infrared Absorption Spectrum of Diopside," *Am. Mineral.*, **56** 1607-16 (1971).
13. R. Chen, Y. Wang, Y. Hu, Z. Hu, and C. Liu, "Modification on Luminescent Properties of SrAl₂O₄:Eu²⁺, Dy³⁺ phosphor by Yb³⁺ ions doping," *J. Lumin.*, **128** 1180-4 (2008).
14. C. J. Jeon, W. J. Yeo, and E. S. Kim, "Effect of Crystallization on Thermal Conductivity of Diopside," *J. Ceram. Soc. Jpn.*, **118** 1079-82 (2010).
15. A. Karamanov and M. Pelino, "Evaluation of the Degree of Crystallisation in Glass-Ceramics by Density Measurements," *J. Eur. Ceram. Soc.*, **19** 649-54 (1999).
16. S. Y. Choi, D. H. Lee, D. W. Shin, S. Y. Choi, J. W. Cho, and J. M. Park, "Properties of F-Free Glass System as a Mold Flux: Viscosity, Thermal Conductivity and Crystallization Behavior," *J. Non-Cryst. Solids*, **345-6** 157-60 (2004).
17. C. Clauser and E. Huenges, "Thermal Conductivity of Rocks and Minerals," pp. 105-26 in *Rocks Physics and Phase Relations- a Handbook of Physical Constants*, AGU Reference Shelf, Vol. 3, Ed. by T. J. Ahrens, American Geophysical Union, Washington, DC, USA, 1995.